ENERGY EQUIPSYS

Energy Equipment and Systems

www.energyequipsys.com

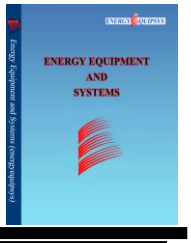

Performance assessment of a hybrid fuel cell and micro gas turbine power system

Ahmad Tahmasebi [a]
Ahmad Sedaghat [b*]
Rasool Kalbasi [a]
Mahdi Moghimi Zand[c]

[a] Islamic Azad University, Najafabad Branch, Najafabad, I.R. of Iran

[b] Department of Mechanical Engineering, Isfahan University of Technology, Isfahan 84156-83111, I.R. of Iran

[c] School of Mechanical Engineering, College of Engineering, University of Tehran, P.O.Box 11155-4563, Tehran, Iran

ABSTRACT

In this paper, a hybrid solid oxide fuel cell (SOFC) and micro gas turbine (MGT) power system is parametrically studied to evaluate the effect of different operating conditions. The SOFC/MGT power system includes SOFC reactor, combustion chamber, compressor and turbine units, and two heat exchangers. The effects of fuel utilization, temperature, and pressure are assessed on performance of the hybrid SOFC/MGT power system using energy and exergy analyses. This study reveals that the main exergy loss occurs in the external reformer and the maximum achievable output power is about 7kW for the hybrid system. Finally, the promising first law thermal efficiency of up to 83% is achieved when the second law efficiency enhances to 65% for the hybrid system.

Article history:

Received 21 May 2013
Accepted 15 June 2013

Keywords: Energy & Exergy, Micro Gas Turbine, Solid Oxide Fuel Cell, Thermal Efficiency.

1. Introduction

The demand for power-generation systems of high efficiency with low emission is of increasing importance. Recently, the fuel cell (FC) has been regarded as an enabling clean energy technology with great potential worldwide because it can convert the chemical energy of the fuel directly to energy; therefore, they can theoretically achieve high electrical efficiency. Fuel cells produce very low levels of pollutant emissions such as NOx, SOx, and CO_2. They are also amenable to high-volume production as standardized power modules.

Over the years many types of fuel cells have been developed with their names based on the type of electrolyte utilized. The first type of cells was known as phosphoric acid fuel cells (PAFC).

*Corresponding author:
Department of Mechanical Engineering, Isfahan University of Technology, Isfahan 84156-83111, I.R. of Iran
E-mail address: sedaghat@cc.iut.ac.ir, (Ahmad Sedaghat)

These cells used a phosphoric acid electrolyte and platinum electrodes.The problems encountered with these cells included leakage of the electrolyte and the high cost of platinum electrodes. The next type of cells was known as the molten carbonate fuel cell (MCFC). These cells use a molten salt as an electrolyte and operate at 600°C. The type of cell presently under development is the proton exchange membrane fuel cell (PEM). These cells have an acidic electrolyte in a polymer matrix and are presently being sought by the automobile industry to produce electric hybrid vehicles. The latest type and probably the best suited for central power generation is the solid oxide fuel cell (SOFC). These cells use a solid ceramic electrolyte of yttria zirconia which the operating temperature ranges from about 600 to 1000 °C [1].

An important advantage of a high-temperature fuel cell is the high temperature exhaust gas which can be used as an additional heat source for other purposes. With combining a gas turbine cycle (GT) to a high temperature fuel cell, a hybrid cycle is formed and the

outlet exergy is recovered and the thermal efficiency is enhanced. The theoretical feasibilities of such hybrid power systems have been investigated by numerous research groups. Several SOFC based power generation systems developed by Siemens-Westinghouse were simulated using the developed SOFC stack model [2]. Veyo and Lundberg [3] showed that an atmospheric pressure SOFC based power generation cycle has an thermal efficiency range of 45%-50% and the SOFC and gas turbine hybrid cycle can provide up to 70% of electrical efficiencies [3]. For small scale electrical power generation with a range of 250kW, a thermal efficiency of 65% can be expected [4]. In general, simplified or empirical, mathematical or validated model are used to predict the behavior of hybrid fuel cell and gas turbine. Stephenson and Richey [5] used simplified and empirical relation based on performance curves from Siemens-Westinghouse. Lunghi and Umbertini [6] used a mathematical model with detailed electrochemical loss description, simplified assumption of uniform cell and gas temperature and current density. Some advanced fuel cell models are utilized by Harvey and Richey [7] and Costamagna and Massardo [8]. Some studies such as Companari [9], Johansson [10], Lunghi and Umbertini [6] focused on relatively large systems allowing for higher pressure ratio and intercooled and reheated gas turbine. But smaller systems is studied moderate inlet conditions by Campanari [11] and Magistri [12].

In this study, a combined SOFC and micro gas turbine are considered. This system is designed based on in town natural gas utilities. With electrochemical and thermodynamic properties of SOFC and distinguishing different losses in SOFC, the SOFC current density during the process. The generated heat of reheated gas partly dissipated to the which combine SOFC with a microturbine with and cell voltage are calculated. The effects of temperature, pressure, and fraction of reactant gases as major parameters, cell dimension and proportion of generated power in each section as minor parameters are investigated at different working conditions.

2. System Configurations

A schematic diagram of the tubular SOFC/MGT hybrid power system is given in Fig.1. Although solid oxide fuel cells can be fed by a number of fuels (methane, natural gas, biogas, syngas, etc.), methane at ambient temperature is considered here as the fuel. The compressed fuel (methane) is heated in heat exchanger and then reformed by using steam and heat from the fuel cell. In the reformer, the following reaction is reported:

$$CH_4 + H_2o \rightarrow Co + 3H_2 \quad \& \quad Co + H_2o \rightarrow Co_2 + H_2$$

The reformer productions are fed to anode section of SOFC. Ambient air is compressed by a turbine driven compressor and then heated in the heat exchanger by the hot gas stream from the turbine exhaust. The hot, high-pressure air is then fed to the cathode. Natural gas and air are channeled through the anode and cathode compartments, respectively.

The electrochemical reaction occurs and electrical energy is produced associated with heat generation reform environment, partly used to the natural gas and partly used to heat up the feedstock gases.

The high-temperature productions and unused gases, which compound of unutilized reformed natural gas and depleted air, are guided to a combustor where residual fuels (hydrogen, methane and carbon monoxide), reacts with the excess air. The combustion productions with high temperature and pressure are

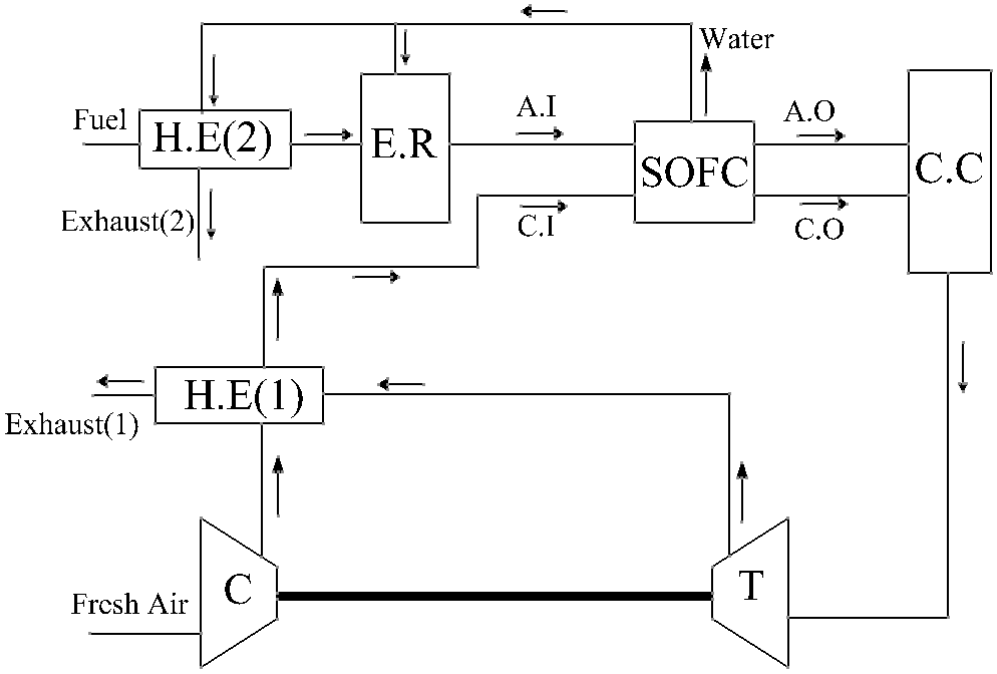

Fig.1. Schematic diagram of the tubular SOFC/MGT hybrid power system.

channeled to turbine. In turbine, expansion occurred and thermodynamic properties such as pressure and temperature are reduced. The specification of hybrid system components are given in Table 1. The turbine outlet has high temperature and it can be used for increasing of compressor outlet in heat exchanger (1).

The following assumption has been made in modeling:

(a) all components are adiabatic,
(b) uniformity of temperature within all components,
(c) feeding cathode stream is composed of O_2 and N_2, while feeding anode is CH_4, CO, CO_2, H_2 and H_2O
(d) Fuel cell electrochemical reaction is as

$$\frac{1}{2}O_2 + 2e^- \rightarrow O^{-2} \quad Cathode$$

$$H_2 + O^{-2} \rightarrow H_2O + 2e^- \quad anode$$

$$H_2 + \frac{1}{2}O_2 \rightarrow H_2O \quad Overall\,reaction$$

(e) The electrochemical reaction of CO has not been taken into account
(f) Temperature of gases stream at the outlet of the reformer and SOFC stack are equal to the reformer and stack temperature, respectively.
(g) Gases do not leak outside from the system;
(h) Chemical reactions proceed to equilibrium states
(i) steady-state operation is achieved;

3. Electrochemical Potential

For any power producing device a maximum work potential is defined for that system. For the fuel cell system, the maximum work potential is known as the electrochemical potential. For a simple cell operating reversibly in steady state at constant pressure and temperature, the first law of thermodynamics is expressed by:

$$H_i - H_o + Q - W = 0 \tag{1}$$

where H_i and H_o represent the entering and exiting enthalpies, respectively. Q represents the input heat and W the output work. The second law of thermodynamics can be written as

$$S_i - S_O + \frac{Q}{T} + S_{gen} = o \tag{2}$$

where S_i and S_o represent the entering and exiting entropies, respectively. For a reversible system, the entropy generated is zero and the heat transfer can be expressed by:

$$Q = T(S_o - S_i) \tag{3}$$

Substituting (3) into (1) and realizing that a reversible system produces the maximum work:

$$\begin{aligned} &H_i - H_o + T(S_o - S_i) - W_{\max} = 0 \\ &\rightarrow W_{\max} = (H_i - TS_i) - (H_o - TS_o) \\ &\rightarrow W_{\max} = -\Delta G \end{aligned} \tag{4}$$

Therefore to calculate the cell's maximum potential voltage, the change in the Gibbs' free energy is necessary to be known for the overall reaction, also this amount is equal to *2EF*, then

$$W_{\max} = 2EF \rightarrow E = \frac{W_{\max}}{2F} \tag{5}$$

where the number 2 in (5) represents the number of electrons, E is the maximum voltage (reversible voltage) obtainable, and F is the Faraday constant.

3.1. Overpotentials in SOFC

In general, fuel cell achieves its maximum reversible voltage in case of no current imposed by the external load. Due to irreversibility in the cell operation, the cell voltage, V, is always lower than reversible voltage E. This difference termed polarization and is the sum of three types of losses including, activation, ohmic and concentration.

3.1.1. Activation Losses

Kinetics of electrochemical reactions is measured by the current density. Both anode and cathode semireactions must be catalyzed, supplying some additional energy in order to speed up the overall electrochemical reaction.

This energy, i.e. the activation energy, is usually measured by the overpotential, which is the difference

Table 1. Specification of the hybrid SOFC/MGT system.

Fuel Inlet Temperature (°C)	20	SOFC Temperature (°C)	800
Fuel Inlet Pressure (kpa)	300	SOFC Pressure (kpa)	300
Air Inlet Temperature(°C)	20	Number Of Cells	120
Air Inlet Pressure (kpa)	100	Cell Area (cm^2)	130
External Reformer Efficiency (%)	80	Combustor Isentropic Efficiency (%)	98
Internal Reformer Efficiency (%)	80	Combustor Pressure drop (%)	4
Compressor Isentropic Efficiency (%)	87	Air Stoich	6
Turbine Isentropic Efficiency (%)	89		

between equilibrium and non-equilibrium voltage. At equilibrium, the electronation current density, $i^{\rightarrow}$ equals the deelectronation current density, $i^{\leftarrow}$ or the number of ions going from electrode to electrolyte equals the number going from electrolyte to electrode. This equality of charge transfer, which represents a quantitative measure of the rate of reaction, is known as the equilibrium exchange-current density, i_o. These exchange-current densities can vary depending on reaction as well as electrode material and temperature.

The energy barrier between the electrode and electrolyte results in a loss known as activation loss, significant at low currents. The activation overvoltage is calculated using the Butler–Volmer equation [13],

$$i = i_o\left[\exp\left(\alpha\frac{nF}{RT}V_{act}\right)-\exp\left(-(1-\alpha)\frac{nF}{RT}V_{act}\right)\right]$$

$$\Rightarrow V_{act} = \frac{RT}{F}\sinh^{-1}\left(\frac{i}{i_o}\right) \quad (6)$$

, where α is the charge exchange constant and set to the value of 0.5, i_o is the exchange current density which are taken from Costamagna & Hoenegger [14]:

$$i_{o,cathode} = \gamma_{cathode}\left(\frac{P_{O_2}}{P_{ref}}\right)^{0.25}\exp\left(-\frac{E_{act,chatode}}{RT}\right)$$

$$i_{o,anode} = \gamma_{anode}\left(\frac{P_{H_2}}{P_{ref}}\right)\left(\frac{P_{H_2O}}{P_{ref}}\right)\exp\left(-\frac{E_{act,anode}}{RT}\right) \quad (7)$$

3.1.2. Ohmic Losses

Ohmic losses are caused by resistance to the conduction of ions through the electrolyte and the electrons through the electrodes and current collectors and by contact resistance between the cell components. The ohmic losses is calculated from the resistivities of individual layers such as anode, cathode and electrolyte and is given by [15]

$$V_{ohm} = i\sum_j R_j = i\sum_j \frac{A_j\exp(B_j/T)\delta_j}{A_{s,j}} \quad (8)$$

The corresponding coefficients of A, B, δ are given in Table 2 [16].

Table 2. Coefficients used in equation (8) [16].

Component	δ(cm)	B(K)	A(cmΩ)
Anode	0.00298	1392	0.01
Cathode	0.0814	-600	0.19
Electrolyte	0.0094	-10350	0.004
Interconnection	0.1256	-4690	0.0085

3.1.3. Mass Concentration Losses

One of the major losses known to exist in any fuel cell, resulting from mass transfer limitations, is known as concentration polarization. In the ideal case, a fuel cell would obtain a voltage drop equal to the difference in potential between the two electrodes when no current was flowing. At this point the concentration of fuel or oxidant at the respective electrode would be the same as that in the free stream. The concentration loss is given by

$$V_{conc} = \frac{RT}{2F}\ell n\left(1-\frac{i}{i_l}\right) \quad (9)$$

,where i is the current in the fuel cell and i_l is the limiting current in that cell as determined from mass transfer relations [17]. The limiting current density arises from the fact that the maximum achievable current per unit area is limited by the rate at which the fuel or oxidant can reach the reaction sites.

Concentration overpotential becomes significant when large amounts of current are drawn from the fuel

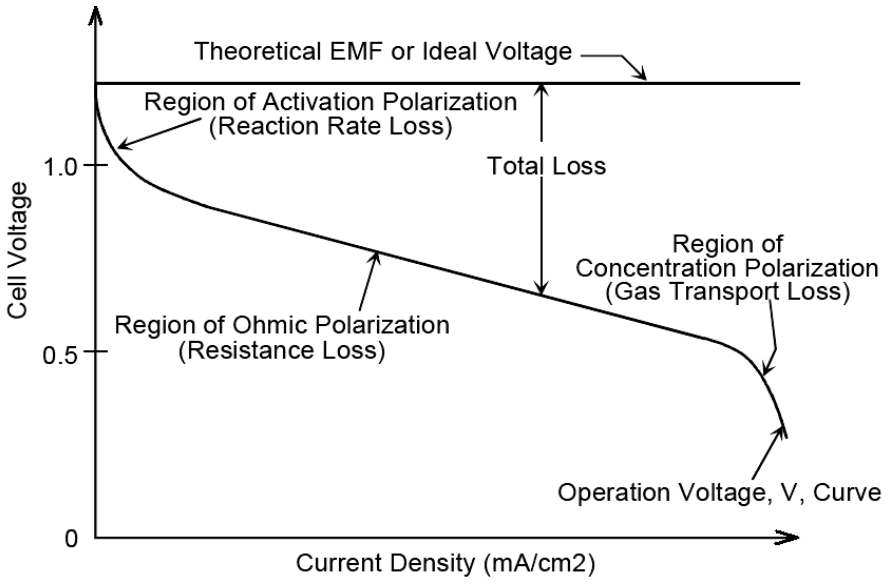

Fig.2. Polarization curve[13].

cell. The partial pressure of the gases at the reaction sites, which corresponds to the volume concentration of the gases, will be less than that in the bulk of the gas stream when a large amount of current is drawn. If such partial pressure or concentration polarization are unsustainable, concentration polarization will cause excessive voltage losses and the fuel cell will cease to operate. All the above mentioned over voltages are evaluated at the outlet SOFC temperature. The overall voltage of the single cell can be calculated as a function of current density, temperature, pressure, chemical composition and geometric/material characteristics by calculating the difference between the reversible potential and the over voltages as shown in Fig.2, i.e. polarization curve. At the high voltages, a slight decrease in voltage does not result in a substantial increase in current density. This is due to the dominance of activation polarization term at high voltages and low current densities. At these high voltages, the majority of energy which would be utilized to increase current density is now utilized to overcome the activation energy barrier. Below O.9V, the current density increases fairly linearly with a decrease in voltage due to the dominance of ohmic loss term. Below O.5V the linear trend breaks down and the increases in current density are much less for continued decreases in operating voltage. This trend is due to the concentration polarizations or mass transfer limitations increasing dramatically. Therefore the cell voltage can be calculated as follows:

$$V_{cell} = E - V_{\text{ohm}} - V_{\text{concetration}} - V_{\text{activation}} \quad (10)$$

4. System Modeling

4.1. Combustion Chamber Model

Since the fuel utilization factor [13, 18] is usually lower than 85%, hydrogen molar flow at SOFC outlet is not negligible. In the combustor, hydrogen and in lower percentages carbon monoxide and methane are available. The oxidant is the depleted oxygen of the cathode outlet stream. The air mass flow rate is much higher than the fuel one in order to control stack temperature. Consequently, oxygen mass flowrate is much higher than the required combustion stoichiometric value. Combustion reactions, assumed at chemical equilibrium and driven into completion, are:

$$\begin{aligned} &CH_4 + 2O_2 \rightarrow CO_2 + 2H_2O \\ &H_2 + \tfrac{1}{2}O_2 \rightarrow H_2O \\ &CO + \tfrac{1}{2}O_2 \rightarrow CO_2 \end{aligned} \quad (11)$$

The combustion chamber is adiabatic and outlet temperature is calculated on the basis of a simple energy balance on the combustor control volume.

4.2. Heat Exchanger Model

As mentioned, the SOFC temperature operating range is from about 600 to 1000 °C. Although the overall chemical and electrochemical reactions are largely exothermic, air and fuel must be preheated before entering the stack in order to avoid high temperature gradients. Such processes are performed by means of two tubes in tube counter flow heat exchangers. The heat exchanger performs two-sided energy and mass flow rate balances. The energy balances for the hot and cold fluids are expressed by:

$$\begin{aligned} &m_{cold}(H_{out} - H_{in})_{cold} - Q_{leak}) - \\ &(m_{hot}(H_{in} - H_{out})_{hot} - Q_{loss}) = 0 \end{aligned} \quad (12)$$

The total heat transfer between the tube and shell sides (heat exchanger duty) can be defined in terms of the overall heat transfer coefficient, the area available for heat exchange, and the log mean temperature difference:

$$Q = UA\Delta T_{LM} F_t \quad (13)$$

These devices are simulated on the basis of the $\varepsilon - NTU$ method [19], implementing temperature-dependent specific heats.

4.3. Turbomachineries Model

The centrifugal compressor operation is used to increase the pressure of an ideal gas stream with relative high capacities and low compression ratio. The turbine operation is used to decrease the pressure of a high pressure inlet gas stream to produce an outlet stream with low pressure and velocity. For a centrifugal compressor, the isentropic efficiency is given as the ratio of the isentropic (ideal) power required for compression to the actual power required:

$$Efficiency_{\ Compressor}(\%) = \frac{power\ required_{isentropic}}{power\ required_{actual}} \times 100\% \quad (14)$$

For the turbine, the efficiency is given as the ratio of the actual power produced in the expansion process to the power produced for an isentropic expansion:

$$Efficiency_{turbine}(\%) = \frac{power\ produced_{actual}}{power\ produced_{isentropic}} \times 100\% \quad (15)$$

In general, the input or output work for a mechanically reversible process can be determined from:

$$W = \int V\, dp \quad (16)$$

With simplification, the required work for compressor or the produced work by the turbine is calculated by [19]:

$$W = F_1(MW)\left(\frac{n}{n-1}\right)CF\left(\frac{P_1}{\rho_1}\right)\times\left[\left(\frac{p_2}{p_1}\right)^{\left(\frac{n-1}{n}\right)} - 1\right] \quad (17)$$

For the centrifugal compressor: Power Required$_{actual}$ = Entalphy$_{outlet}$ –Entalphy$_{inlet}$ and for the turbine, Power produced$_{actual}$ = Entalphy$_{inlet}$ – Entalphy$_{outlet}$. In the case of air compressor, the inlet status corresponds at the

environmental one, whereas temperature and pressure of the GT inlet stream can considerably vary according to the changes in the design and operating parameters. Air compressor and gas turbine are assumed to be coupled on a unique shaft; as a consequence, they must have the same rotor speed.

4.4. SOFC Stack Model

The SOFC stack consists of many single cells to increase the voltage output and hence the electrical power for practical applications. In the SOFC stack model, several parameters such as gas utilization, energy efficiency, thermodynamic properties (pressure, temperature), electric power and interaction between the cells are considered. A complete analysis of energy and mass flow rate are performed in HYSYS software package, and the simulation results are derived. The model considers mass flow rate variation due to chemical reaction such as hydrogen oxidation, methane reforming, and water gas shift reaction of carbon monoxide. The hydrogen and oxygen is consumed and the rest amount of hydrogen and oxygen is obtained from faraday's law. It offers a convenient and time saving means for chemical process studies, including system modeling, integration and optimization. It is used in this study as a process simulation tool to investigate potential SOFC based power generation cycles including SOFC stack and the balance of plants. To facilitate the study, a natural gas feed tabular SOFC stack model is developed using existing HYSYS functions and unit operation models with minimum requirements for linking of a subroutine. This approach fully utilizes the existing capabilities of this process simulator and provides a convenient way to perform detailed process study of SOFC based power generation cycles. The SOFC produced power is:

$$P = nIV_{cell} \tag{18}$$

where n denotes the SOFC cell numbers. Then the net power from the hybrid SOFC/MGT system is determined by

$$P_{net} = P_{sofc} + P_{turbine} - P_{compressor} \tag{19}$$

5. Model Validation

In order to validate the current modeling, different losses are calculated in HYSYS and the results are compared with Calise and his colleagues [20] in Fig.3 to 6.

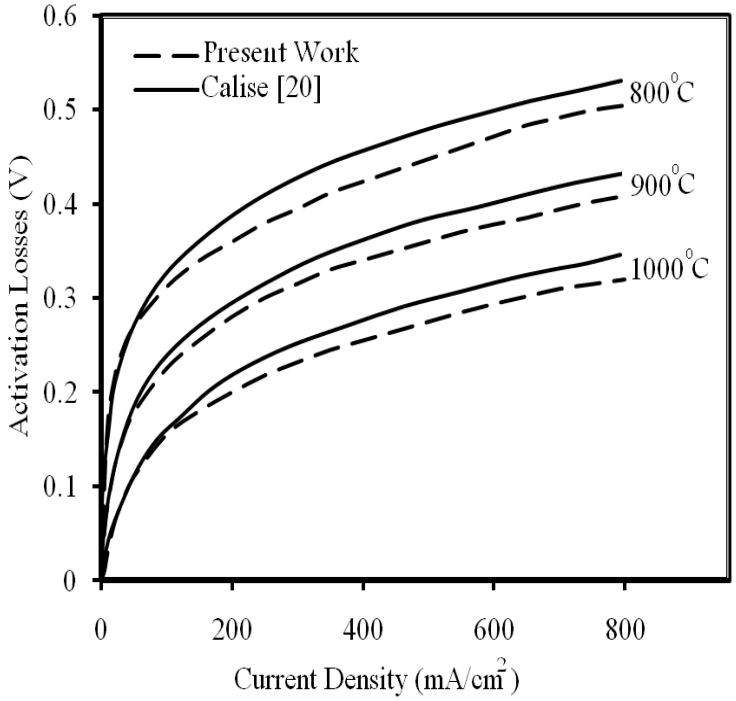

Fig.3. Activation losses comparison between present work and Calise [20].

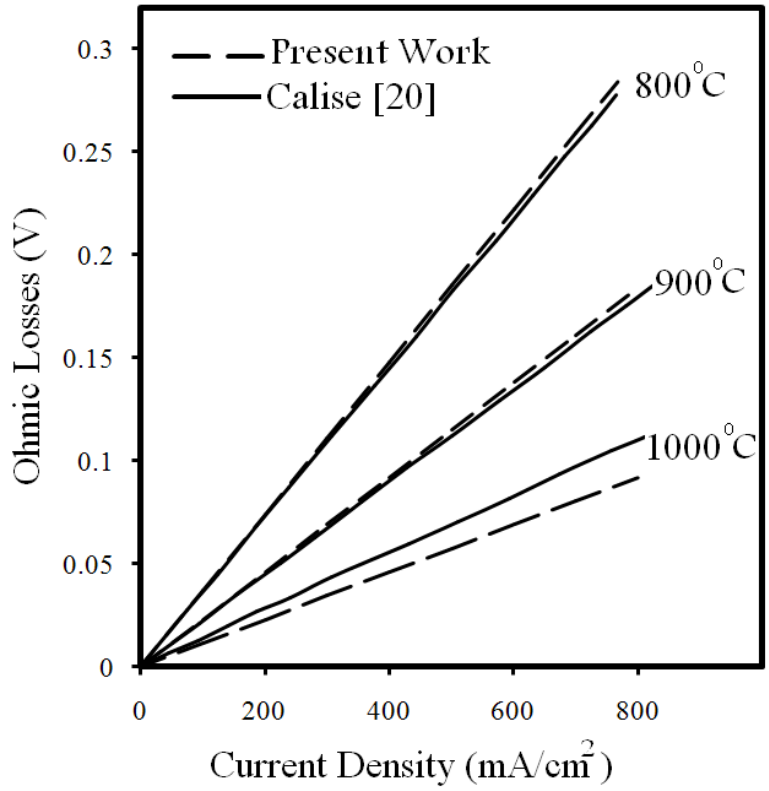

Fig.4. Ohmic losses comparison between present work and Calise [20].

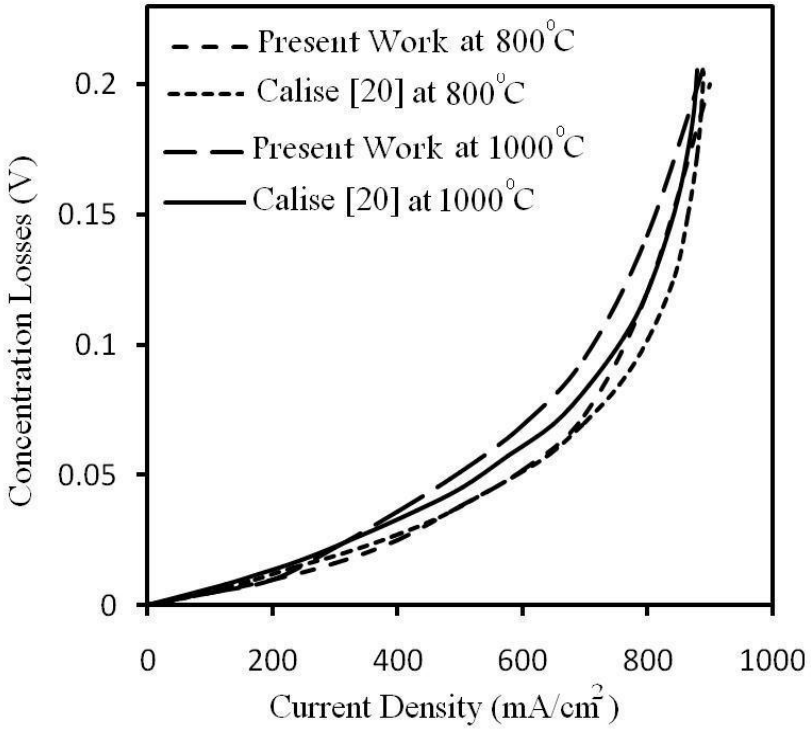

Fig.5. Concentration losses comparison between present work and Calise [20].

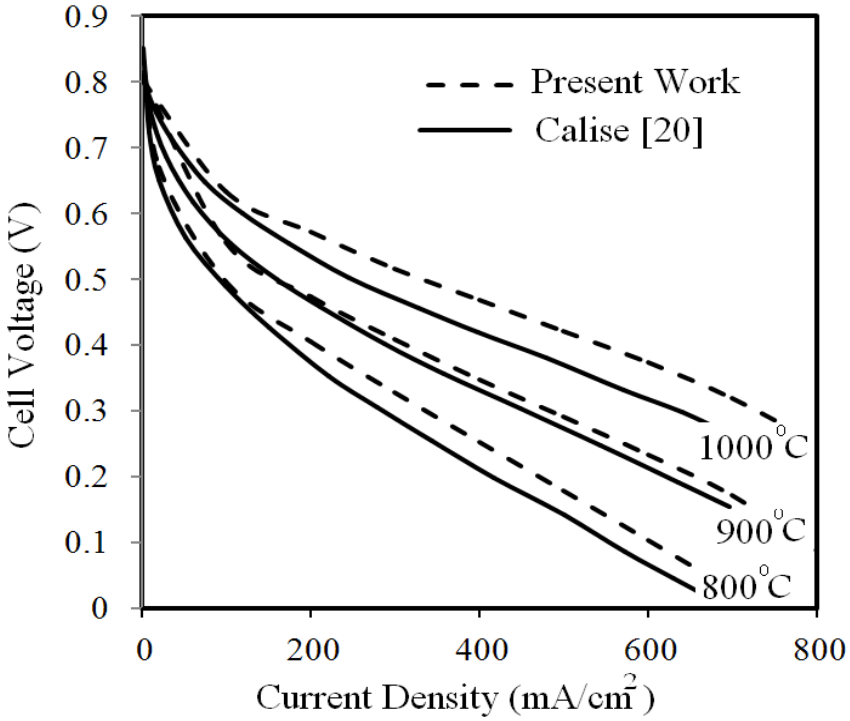

Fig.6. Polarization curve comparison between present work and Calise [20].

6. Exergy Analysis

6.1. Exergy Concept

The second law of thermodynamics has proved to be a very powerful tool in the optimization of complex systems. A system can delivers the maximum possible work as it undergoes a reversible process from the specified initial state to the state of its environment, that is, the dead state. This represents the useful work potential of the system at the specified state and is called exergy. Rather, it represents the upper limit on the amount of device work can deliver without violating any thermodynamic laws.

From the first low of thermodynamic, it is evident that the energy is conserved. Based on conservation of energy principle, energy cannot be created or destroyed during a process. Unlike the energy, exergy is not conserved. For an isolated system during a process always decreases or, in the limiting case of a reversible process, remains constant. In other words, it never increases and exergy is destroyed during an actual process. This is known as the decrease of exergy principle.

Irreversibilities such as friction, mixing, chemical reactions, and heat transfer through a finite temperature difference, unrestrained expansion, nonquasiequilibrium compression or expansion always generate entropy, and in general anything that generates entropy always destroys exergy. The exergy destroyed is proportional to the generated entropy and expressed as following:

$$EX_{destroyed} = T_o S_{gen} \quad (20)$$

, where EX is exergy, S_{gen} is entropy generation and is computed according to entropy balance.

$$S_{in} - S_{out} + S_{gen} = \Delta S_{sys} \quad (21)$$

Also exergy destroyed can be expressed from exergy balance

$$EX_{in} - EX_{out} - EX_{destroyed} = \Delta EX_{sys} \quad (22)$$

Exergy destroyed represents the lost work potential and is also related to the irreversibility [21]. In this study exergy destroyed is calculated from both entropy and exergy balance.

6.2. Exergy Components

Exergy of a stream of matter in the absence of nuclear, magnetism, electricity and surface tension effects, is the sum of

$$EX = EX_{ke} + EX_{pe} + EX_{th} + EX_{ch} \quad (23)$$

In the present study, the changes in the kinetic and gravitational potential energies are considered to be negligible, and then the thermal and chemical exergy are given by:

$$EX_{th} = (H - H_o) - T_o(S - S_o)$$
$$EX_{ch} = \sum_j X_j(\mu_{j0} - \mu_{j00}) \quad (24)$$

where X_j is the mole fraction, μ_{j0} is the chemical potential of the species j which is evaluated at T_0 and P_0, μ_{j00} is the chemical potential which is calculated in the reference environment.

6.3. Exergy Balances

In order to calculate the irreversibility, exergy balance of each component in Fig.1 should be carried out. For heat exchanger and turbomachinery component, destroyed exergy can be obtained from Eq.(25).

For external reformer, SOFC and combustor, the exergy destroyed can be calculated from entropy balance.

$$(\dot{S}_{gen})_{External\,\mathrm{Re}\,former} = -\dot{Q}/T_o + \dot{m}_3 S_3 - \dot{m}_1 S_1 - \dot{m}_2 S_2$$
$$(E_{destroyed})_{External\,\mathrm{Re}\,former} = T_o \dot{S}_{gen}$$
$$\rightarrow E_{destroyed} = -\dot{Q} + T_0(\dot{m}_3 S_3 - \dot{m}_1 S_1 - \dot{m}_2 S_2)$$
$$(E_{destroyed})_{combustor} = T_0(\dot{m}_3 S_3 - \dot{m}_1 S_1 - \dot{m}_2 S_2)$$
$$(E_{destroyed})_{SOFC} = T_0(\dot{m}_3 S_3 + \dot{m}_4 S_4 - \dot{m}_1 S_1 - \dot{m}_2 S_2) + \dot{Q} \quad (25)$$

The destroyed exergy is calculated for each component and listed in Table 3. The inlet exergy is referred to Methane which is entered at 25 °C. Increasing temperature decreases the overpotantial losses and irreversibilities in SOFC; therefore, it improves the overall efficiency as well as the second low efficiency.

7. Parametric Study for the Hybrid System

In this section, the effect of different parameters such as temperature, pressure, cathode and anode molar flow has been studied.

7.1. The Temperature of SOFC

Although the open circuit voltage decreases with increasing temperature according to Eq.(4), the performance at operating current densities increases with increasing temperature due to reduced mass transfer polarizations and ohmic losses.

The dependency of SOFC performance on temperature is illustrated in Fig.6. The sharp decrease in cell voltage as a function of current density at $800^{o}C$ is a result of the high ohmic polarization of the solid electrolyte at this temperature.

The ohmic polarization decreases as the operating temperature increases and correspondingly, the current density at a given cell voltage increases. Increasing the temperature also affects the turbine and its output power will increase. Figure 7a, shows temperature changes on produced power changes of cell. As can be observed increase in cell output power is higher than the gas turbine. So that the cell shares in producing total power in temperatures 800, 900 and 1000 are respectively equal with 50.5%, 59% and 61%.

7.2. The Pressure of Cycle

With increasing of pressure in cycle, the inlet enthalpy of turbine increased and then power produced is improved. Figure 7b shows the produced power in SOFC and turbine if pressure is changed. SOFC fuel cell shows an enhanced performance by increasing cell pressure. The effects of pressure of the cell voltage are also shown in Fig.8 favorably improving yield of the cell at higher current densities.

Table 3. Destroyed exergy in each component.

Temperature (°C)	Inlet Exergy (kW)	Destroyed Exergy (kW)							Outlet Exergy (kW)	Second Low Efficiency (%)
		Reformer	Compressor	Turbine	SOFC	Combustor	Heat Exchanger 1	Heat Exchanger 2		
$800\,^{o}C$	8.513	1.073	0.07975	0.07492	0.2474	0.8438	0.04128	0.3584	0.7392	65
$900\,^{o}C$	8.513	1.082	0.07978	0.07504	0.1065	0.7847	0.04673	0.3413	0.678	75.8
$1000\,^{o}C$	8.513	1.09	0.07980	0.0848	0.0857	0.7354	0.0521	0.3136	0.6253	76.5

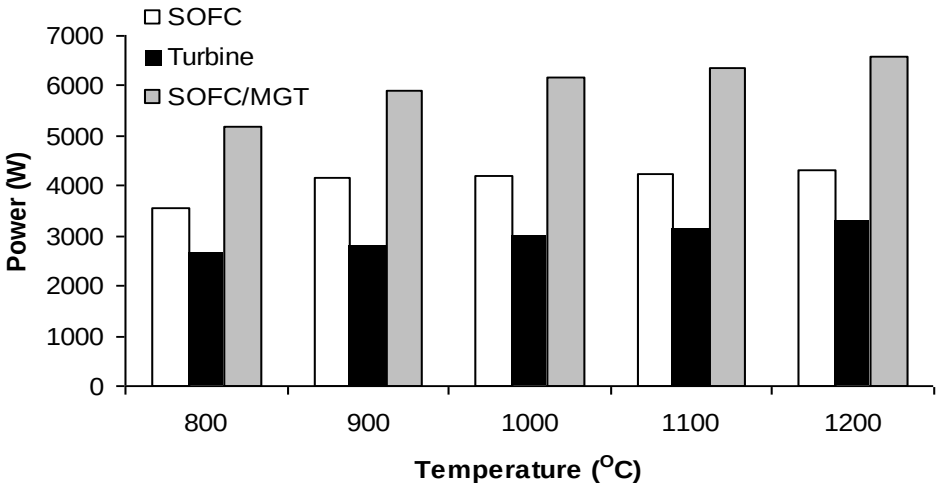

(a)

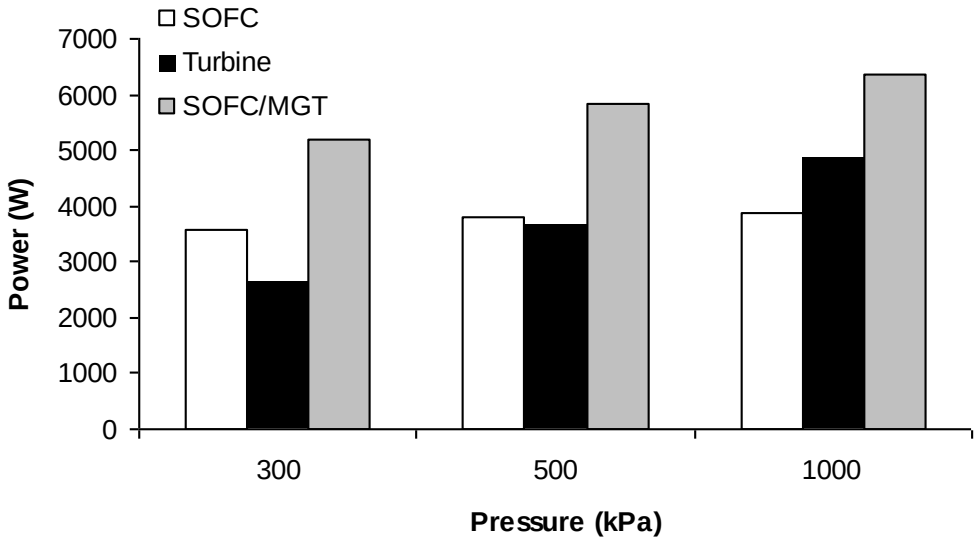

(b)

Fig.7. Power produced by SOFC, turbine, and SOFC/MGT at different: (a) temperatures; (b) pressures.

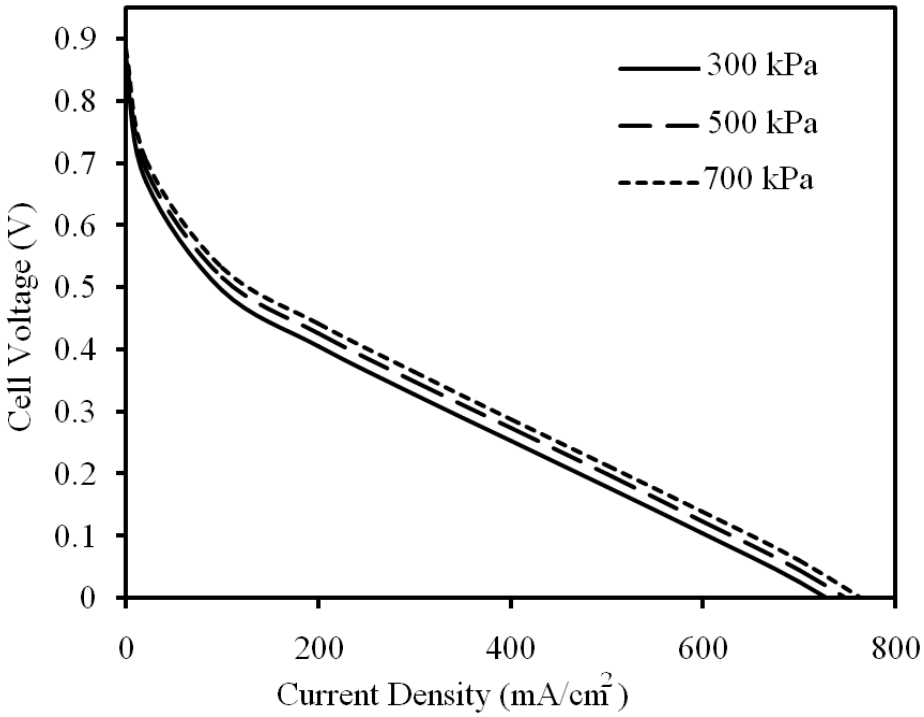

Fig.8. Polarization curve at different current density.

7.3. The Mass Flow Rate

Another design variable which can impact the overall performance of the fuel cell is the Mass flow rate (the current density of the fuel cell). The purpose of this section is to observe the effects of changing one or both of the gaseous flow rates entering the cell. Figure 9, shows the current density effects on the produced power and on the first and second law efficiencies.

7.3.1. The Mass Flow Rate of Fuel

Figure 9a, also shows the power curves for different fuel molar rates, since the fuel molar rates are dependent on current densities, for the SOFC, turbine, and the combined SOFC/MGT systems.

The flow rate of air was varied to provide six times the stoichiometric amount needed to react all of the fuel. By increasing the fuel mass flow rate, the output current value of the fuel cell increases and thus

activation, ohmic and concentration losses increase and cell voltage and therefore output power of the cell will be reduced. Second law efficiency in this case because of the cell entry to the concentration drop region will find a large reduction. By increasing the fuel flow rate and therefore flow rate passing through the turbine, the power will increase.

Figure 9b shows a drop in both first and second low efficiency with increasing mass flow rates. The decrease in efficiency can be explained by a review of the over potential losses. It was shown that increases in flow rate actually showed a decrease in output power. With increases in flow rate, both the air and fuel blowers were required to move more gas resulting in larger size, higher cost, and a greater amount of work required. This increases in parasitic power along with a decrease in output power results in a lower overall efficiency. Likewise, the increase in size and cost of all components of support equipment drives the cost of each kilowatt of electrical power. What cannot be seen from this figure is the environmental impact. With no gains in power for increases in mass flow rate, the exhaust stream becomes rich in hydrogen, carbon monoxide, and oxygen resulting in more products being combusted. Since one of the advantages of a fuel cell is its improved emissions over a normal combustion power cycle, higher flow rates are determined from both emissions and efficiency standpoint.

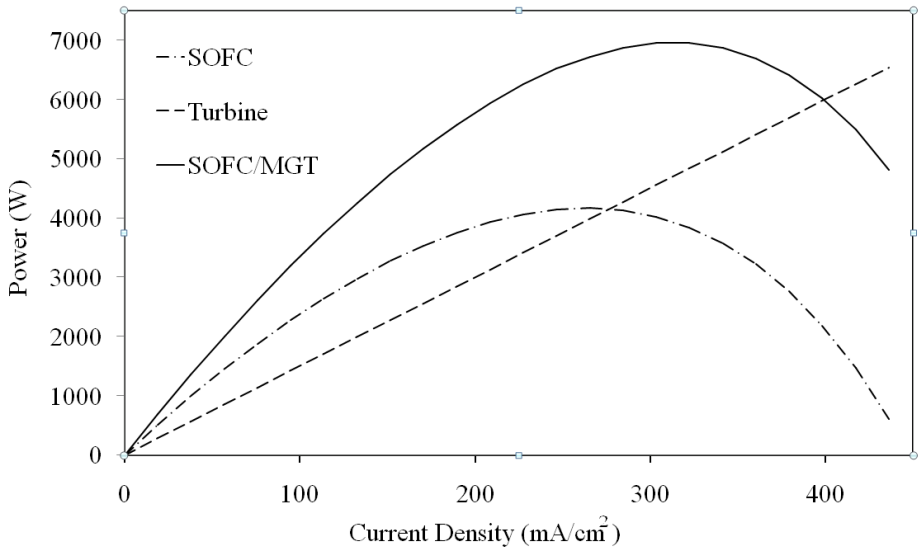

(a)

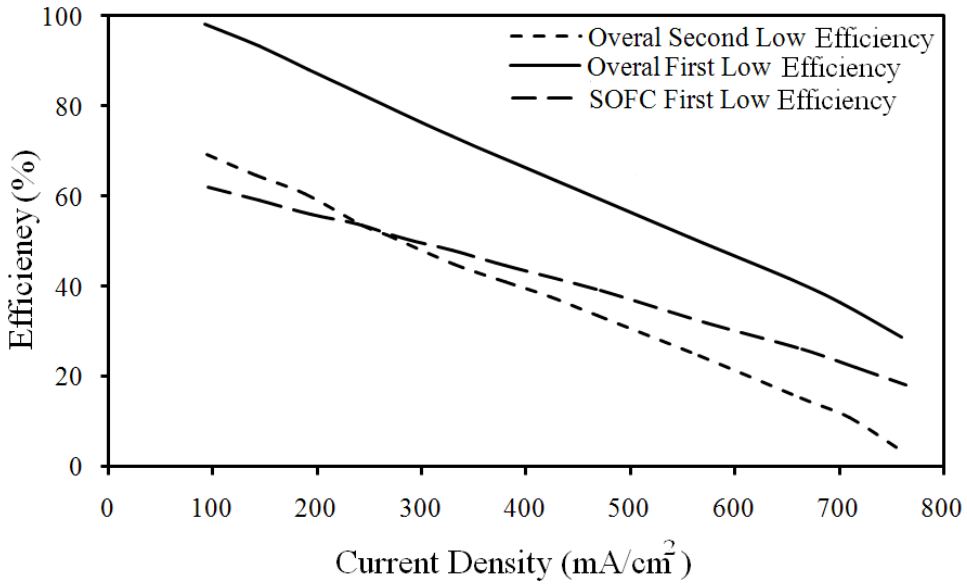

(b)

Fig.9. (a) Power and (b) efficiency produced by SOFC/MGT at different current densities.

7.3.2. The Mass Flow Rate of Air

With increasing air flow due to increasing of partial pressure of cathode, activation losses area reduces. By reducing irreversibility of activation region, the output fuel cell voltage and power increases. Also with increasing air flow rate, flow rate passing through the turbine increases. By increasing the mass flow rate passing through the turbine, the output power will increase. Figure 10a, shows output power in terms of current density (mass flow rate of the fuel cell). Also first and second law efficiencies are shown in Fig.10a. Due to increased output power, first law efficiency increases and due to constant entry exergy and reduction of fuel cell losses, second law efficiency increases.

7.4. Effect of Fuel Utilization in Power Produced

Using internal reformer and also high porosity materials in the cell have extremely positive effect on the cell function. In Fig.10b the power output in SOFC and Turbine based on fuel utilization are compared. As it is apparent from the diagram, increasing the ability to use fuel causes the increase of current density and of course the output power will increase. And while the increase in fuel consumption by cell, the amount of output hydrogen is reduced and therefore the output of combustion area temperature will reduce. By decreasing the entrance temperature of turbine, the output power will decrease. But the Fig.10b reveals that by increasing the consumption of hydrogen in the cell, the total produced power in system will not change. It seems that increasing the fuel cell power and decreasing the produced power in the turbine are neutralizing their effects.

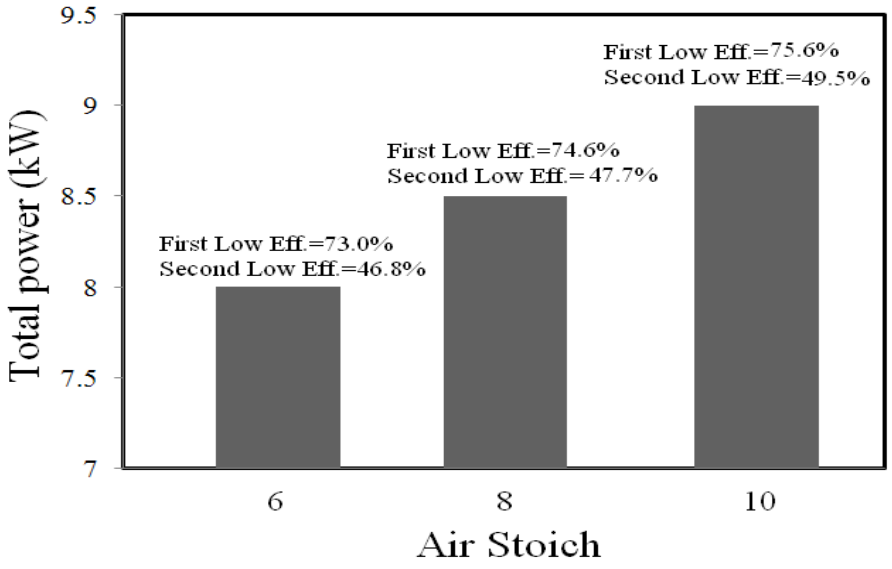

(a)

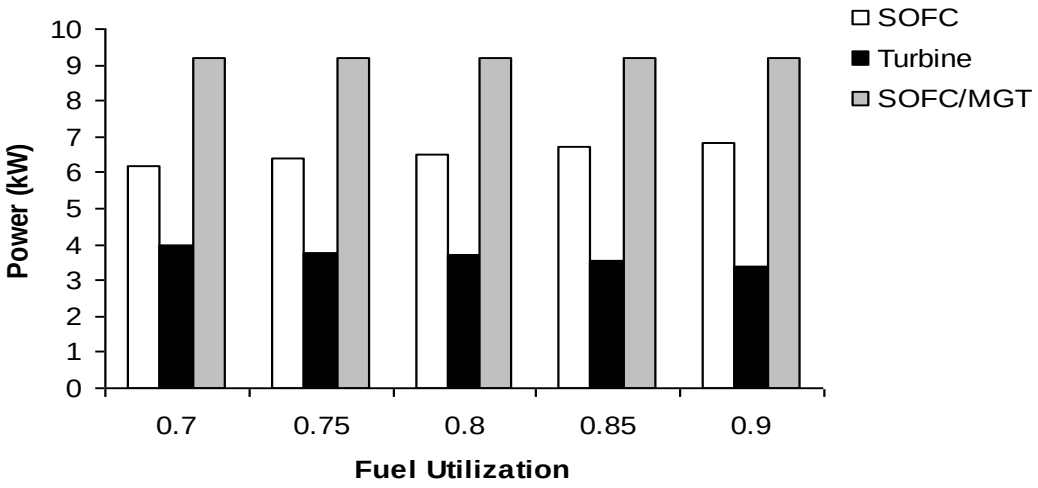

(b)

Fig.10. Effect of air and fuel utilization on power produced.

8. Maximum Output Power of the Combined System

By drawing efficiency based on the total output power of the system, the maximum output power level will be obtained. Figure 11 shows these changes. As observed with increasing the output power, the efficiency is decreased. Maximum output power is estimated to be around 7 kW. The Maximum power is close to the concentration losses region. It is dangerous to approach this region because upon arrival to this region the cell control will be lost .Here with depicting the Grossman diagram for the system in design point (Fig.12) and by considering the input exergy in basis 100, the better illustration for exergy analysis is presented. As Fig.12 represents, the second law efficiency of system is calculated 65%. The most exergy losses are seen in external reforming due to endothermic chemical reactions in this part of system. Also using heat exchangers caused reduction in exergy losses from 3.689 kW to 0.7392 kW.

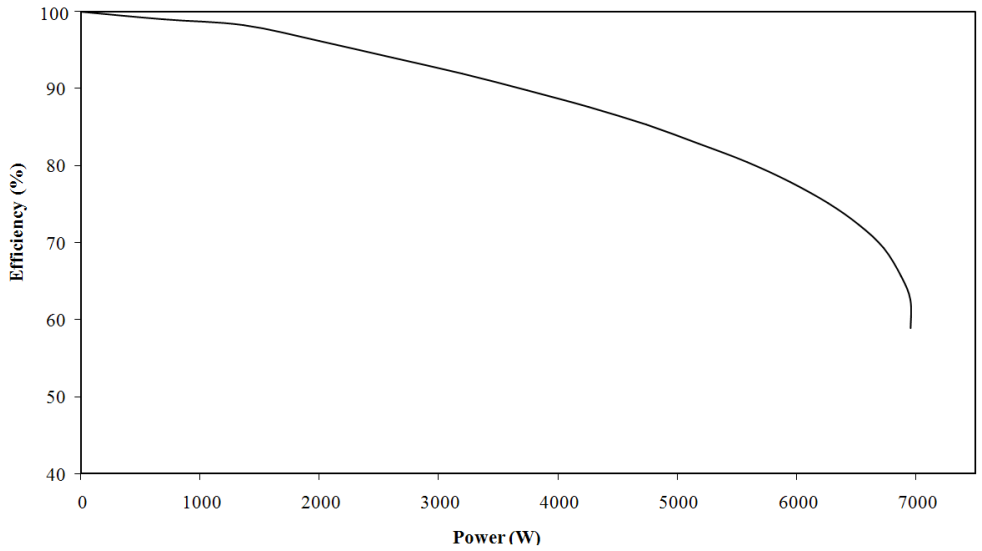

Fig.11. The efficiency versus power.

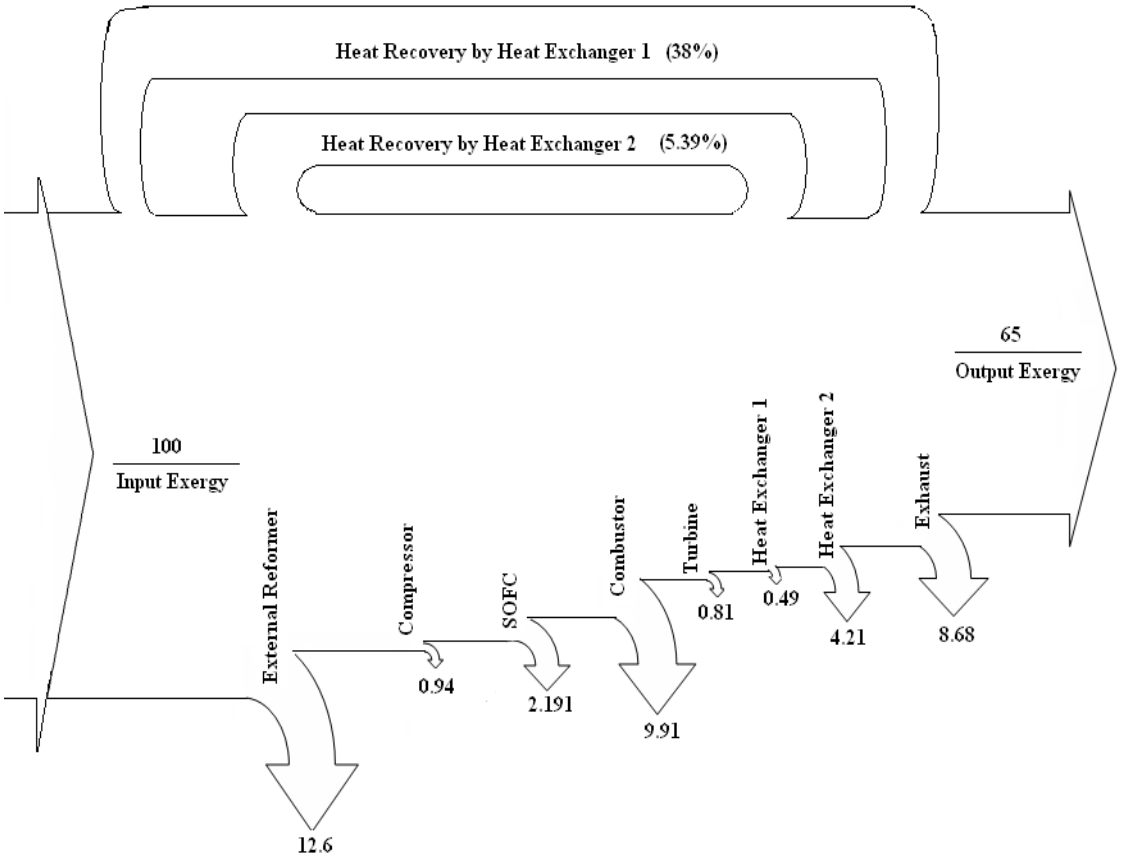

Fig.12. Grossman diagram for the system in design point.

9. Conclusion

In this paper, a parametric study was conducted to assess the effects of different parameters on performance of a hybrid SOFC/MGT power system. The parameters studied include temperature, pressure, the cathode flow rate, the anode flow rate, and percentage of fuel use. Using energy and exergy analyses, the power production and the first and second law efficiencies of the hybrid SOFC/MGT system were determined. The first and second law efficiencies are calculated and the proportion of the power produced by each component of the hybrid system was evaluated. It is observed that, the main exergy loss occurs in the external reformer. Further finding is that the maximum achievable output power from the hybrid SOFC/MGT system is approximately about 7kW. Moreover, the thermal efficiency of the hybrid SOFC/MGT system can be increased to 83% while avoiding critical conditions. Detecting the external reformer as the component which destroys more amount of exergy, the second law efficiency is calculated to be 65% for the hybrid SOFC/MGT system.

Nomenclature

A	heat transfer area (m2)
A.I	Anode Input
A.O	Anode Output
C	Compressor
C.C	Combustion Chamber
C.I	Cathode Input
C.O	Cathode Output
Cp	Heat specific capacity ($kJ.kg^{-1}.K^{-1}$)
E	Open circuit reversible potential (V)
E.R	Enternal Reformer
E_{act}	Activation energy ($kJ.kmol^{-1}$)
F	Faraday constant ($As\ mol^{-1}$)
G	Gibbs free energy ($kJ.kmol^{-1}$)
H.E (1)	Heat Exchanger (1)
H.E (2)	Heat Exchanger (2)
i	current density ($mA.cm^{-2}$)
i_L	limiting current density ($mA.cm^{-2}$)
i_o	Exchange current density ($mA.cm^{-2}$)
M	chemical potential ($kJ.kmol^{-1}$)
m	mass flow rate ($kg.s^{-1}$)
P	electrical power (kW)
p	pressure (bar)
Q	Heat (kJ)
?	area specific resistance ($\Omega.cm^{-2}$)
T	temperature (K), Turbine
U	heat transfer coefficient ($kW.m^{-2}.K^{-1}$)
U_f	fuel u?ilization factor
V	cell potential (V)
V_{act}	activation overpotential (V)
V_{conc}	concentration overpotential (V)
V_{ohm}	ohmic overpotential (V)
W	Work (kJ)
X_i	component molar fraction

Greek Symbols

ΔT_{LM}	Mean logarithmic temperature
δ	component thickness (cm)
η	Efficiency
ρ	density (kg/m^3)

Subscripts

act	Activation
i	Inlet
o	Outlet
ref	reference

References

[1] Appleby, A. and Foulkes, F., A Fuel Cell Handbook, 2nd, Keiger Publishing Co, Florida, 1993.

[2] K. Hassmann, SOFC power plants, the Siemens Westinghouse approach, Fuel Cells 1 (2001) 1.

[3] Veyo S.E., Lundberg W. (1999) "Solid oxide fuel cell power system cycles" ASME Journal, 99-GT-356.

[4] S. campanari, fuel load and part load performance prediction for integrated SOFC and microturbine system, J. Eng. Gas Turbine Power 122 (2000) 239-246.

[5] Stephenson, D. and Ritchey, I., "parametric Study of Fuel Cell and Gas Turbine Combined Cycle Performance", Proceeding of ASME, 97-GT-340, 1997.

[6] Lunghi, P. and Ubertini, S., "Solid Oxide Fuel Cells and Regenerated Gas Turbines Hybrid Systems; a Feasible Solution for Future Ultra High Efficiency Power Plants" Proceeding of the Electrochemical Society, SOFC-VII, Tsukuba, Japan, 2001.

[7] Harvey, S.P and Richter, H.J., "Gas Turbine Cycles with Solid Oxide Fuel Cells parts I and II" Journal of Energy Resources Technology, Vol. 116, 1994.

[8] Costamagna. P., Massado, A. and Bedont, P., "Techno-Economical Analysis of SOFC Reactor-Gas Turbine Combined Plants", Proceeding of the fourth European Solid Oxide Fuel Cell Forum, Lucerne, Switzerland, July, 2000.

[9] Campanari, S. and Macchi E., "thermodynamic Analysis of Advanced Power Cycles Based upon Solid Oxide Fuel Cell, Gas Turbine and Rankine Bottoming Cycles", ASME Conference, 98-GT-585. Stockholm, Sweden, 1998.

[10] Johansson, K., Bafalt, M. and Palsson, J., "solid Oxide Fuel Cells in Future Gas Turbine Combined Power Plants", 22nd CIMAC International Congress on Combustion Engines, 1998, Copenhagen, Denmark.

[11] Campanari, S., "Full load and part load performance prediction for integrated SOFC and microturbine systems", proceedings from ASME, 99-GT-065, Indianapolis, USA, 1999.

[12] Magistri, L., Massardo, A., Rodgers, C. and McDonald, C., "A Hybrid System Based on a personal Turbine (5kW) and a SOFC Stack: A Flexible and High Efficiency Energy Concept for the Distributed Power Market", Proceeding of ASME TurboExpo 2001, 2001-GT-0092, New Orleans, Louisiana, Usa, June, 2001.
[13] Larminie, J. and Dicks, A., Fuel Cell Systems Explained, John Wiley, NewYork, 2000.
[14] Costamagna P, Hoenegger K. Modelling of solid oxide heat exchanger integrated stacks and simulation at high fuel utilization.J Electrochem Soc 1998;145(11).
[15] Calise, F., Dentice d'Accadiaa, M. Palomboa A. and Vanolib, L. "Simulation and exergy analysis of a hybrid Solid Oxide Fuel Cell (SOFC)–Gas Turbine system", Journal of power sources, Vol.158, pp. 225-244, 2006.
[16] S.H. Chan, H.K. Ho, Y. Tian. " Multi-level modeling of SOFC–gas turbine hybrid system", International Journal of Hydrogen Energy 28 (2003) 889 – 900.
[17] Chan,S. and Tian, Y. "Multi-level modeling of SOFC–gas turbine hybrid system", International Journal of Hydrogen Energy 28, 2003.
[18] S.C. Singhal, K. Kendall, High temperature Solid Oxide Fuel Cells,Elsevier, 2003.
[19] Aspen Tech, User Documentation for Aspen Plus, Version 10.1, Cambridge, Massachusetts, USA, 2000.
[20] Calise, F., Dentice d'Accadiaa, M. Palomboa A. and Vanolib, L. "Simulation and exergy analysis of a hybrid Solid Oxide Fuel Cell (SOFC)–Gas Turbine System", Journal of power sources, Vol.158, pp. 225-244, 2006.
[21] Wark, K., Advanced thermodynamics for engineers, McGraw-Hill, New York, 1995.